BG Pulse Journal USA
ISSN:1947-2536 http://www.bgpulseusa.com/index.php/bg
BG PULSE JOURNAL

UDC: 611.018.46:611-018.74:611.06

MORPHOLOGICAL CHANGES OF THE CEREBELLUM IN ACUTE STRESS: HISTOLOGICAL AND MORPHOMETRIC ASSESSMENT

Akramova Shahzodabonu Baxtiyor kizi

2nd-year Master's student, specialty "Morphology"

Department of Human Anatomy and Operative Surgery with Topographic Anatomy,

Tashkent State Medical University, Tashkent, Uzbekistan

E-mail: Shakhzoda2806@gmail.com ; tel.: +998 91 402 98 04

Scientific supervisor: **U.M. Mirsharapov**, Professor

Doi; https://doi.org/10.5281/zenodo.23192691

Abstract. Acute stress triggers activation of the hypothalamic–pituitary–adrenal and sympathoadrenal systems, and the cerebellum, rich in glucocorticoid receptors, is one of the brain regions exposed to this hormonal surge. *Aim:* to give a histological and morphometric characterization of the cerebellar cortex at different times after a single episode of acute stress. *Materials and methods.* The study used 30 male outbred white rats weighing 180–220 g: a control group (n = 10) and an experimental group (n = 20) subjected to 2-hour supine immobilization and examined 1 h, 24 h, 72 h and 7 days after stress (n = 5 per subgroup). Paraffin sections of the vermis were stained with haematoxylin and eosin, toluidine blue and by the Nissl method; the thickness of the cortical layers, the linear density, soma and nuclear area of Purkinje cells, the optical density of Nissl substance and the proportions of Purkinje cell types were measured. *Results.* Acute stress caused a phase-dependent response: early perivascular and pericellular oedema with thickening of the molecular layer (by 10.0% at 24 h), swelling of Purkinje cell bodies and chromatolysis, followed at 24–72 h by a fall in Purkinje cell linear density (by 19.3%), shrinkage of their bodies and the appearance of hyperchromic and ghost cells. By day 7 most parameters approached control values, but Purkinje cell density remained reduced (by 12.4%). Granule cells were considerably more resistant. *Conclusion.* Purkinje cells are the main target of acute stress in the cerebellar cortex; the interval of 24–72 h is the period of maximal destructive change and a rational window for neuroprotective intervention.

Keywords: acute stress, cerebellum, Purkinje cells, morphometry, immobilization, chromatolysis, oedema, rats.

INTRODUCTION

Modern life exposes people to a constant flow of emotional, physical, chemical and social stressors. In moderate doses stress performs an adaptive function, mobilizing the body's defence systems; however, an excessive or prolonged load turns the same mechanisms into a source of

structural and functional damage [1, 2]. The central nervous system is among the most sensitive targets, because both the regulation of the stress response and the cost of its overactivation are concentrated there.

Exposure to a stressor activates the hypothalamic–pituitary–adrenal axis and the sympathoadrenal system, releasing glucocorticoids, adrenaline and noradrenaline [3]. During short exposure these hormones support adaptation, but their excess disturbs neuronal energy metabolism and ion homeostasis and increases neuronal vulnerability to excitotoxic injury [4]. Most of the experimental work on stress-induced brain damage has concentrated on the hippocampus, prefrontal cortex and amygdala [5], whereas the cerebellum has long remained on the periphery of attention.

This view is changing. Beyond coordinating movement, muscle tone and balance, the cerebellum takes part in cognitive and emotional processing, and its damage produces a recognizable cognitive-affective syndrome [6]. Through reciprocal connections with the hypothalamus, the limbic system, brainstem nuclei and the prefrontal cortex, the cerebellum both receives stress-related signals and modulates the stress response [7]. Experimental work has shown that a cerebellar circuit projecting to the ventral tegmental area is required for the development of stress-dependent depression-like behaviour in mice [8], and in humans an acute psychosocial stressor slows cerebellum-dependent sensorimotor adaptation in proportion to the rise in cortisol [9].

Clinically, cerebellar dysfunction under stress may manifest as unsteadiness of gait, impaired balance, hand tremor and slower motor learning, as well as by anxiety and depressive symptoms; reduced cerebellar volume, abnormal activity and altered connectivity have been reported in patients with major depressive disorder and post-traumatic stress disorder [7]. Knowing which cerebellar structures are damaged first, and how quickly they recover, is therefore of interest for neurology, psychiatry and rehabilitation.

The cerebellum is well equipped to respond to stress hormones: during the neonatal period it shows the highest level of glucocorticoid receptors in the brain [10]. Purkinje cells, the large neurons that form the sole output of the cerebellar cortex [11], combine a high metabolic rate, a massive dendritic tree and intense excitatory input from climbing and parallel fibres, which makes them especially susceptible to energy deficit and calcium overload.

Morphological data on the stressed cerebellum come mainly from models of chronic stress, in which a decrease in the number and size of Purkinje cells has been reported [12]. The early response to a single acute stressor is described far less completely. At the same time, acute stress is known to increase the permeability of the blood–brain barrier [13], and one day of restraint stress already produces ultrastructural damage to brain capillary endothelium [14], suggesting that vascular and oedematous changes may set the stage for neuronal injury. A quantitative description of how these changes unfold over time, and of whether they are reversible, is needed both for understanding the pathogenesis of stress-induced disorders and for choosing the timing of neuroprotective intervention.

The aim of the study was to give a histological and morphometric characterization of the cerebellar cortex of rats at different times after acute immobilization stress and to determine the character and sequence of changes in Purkinje cells and the cortical layers.

MATERIALS AND METHODS

Animals. The study was performed on 30 male outbred white laboratory rats weighing 180–220 g, kept in the vivarium of Tashkent State Medical University at 22 ± 2 °C, relative humidity 60 ± 5% and a 12-hour light/dark cycle, with free access to water and standard chow. Before the experiment the animals were adapted for 7 days and then randomized into a control group (n = 10), not exposed to stress, and an experimental group (n = 20).

Acute stress model. Acute stress was induced by immobilization: the animal was fixed in the supine position in a restricted space for 2 hours. Restraint and immobilization are among the most widely used and reproducible stress models and produce a pronounced activation of the hypothalamic–pituitary–adrenal axis [15]. To minimize circadian fluctuations of hormone levels, all procedures were carried out in the morning (09:00–11:00). Depending on the time elapsed after the end of immobilization, the experimental group was divided into four subgroups of 5 animals each: 1 h, 24 h, 72 h and 7 days.

Tissue processing. At the appointed time the animals were euthanized by decapitation under light ether anaesthesia, and the cerebellum was removed immediately. The material was fixed in 10% neutral buffered formalin, dehydrated in ethanol of ascending concentration and embedded in paraffin. Midsagittal sections of the vermis 5–7 µm thick were stained with haematoxylin and eosin (general structure), toluidine blue (neurons and glia) and by the Nissl method (state of the chromatophilic substance). Lobules IV–VI of the vermis were analysed; the lobules were identified with the help of a stereotaxic atlas [16].

Morphometry. Sections were examined and photographed using a light microscope with a digital camera and image analysis software at ×100 and ×400. For each animal three sections and ten non-overlapping fields of view were analysed, following the principles of medical morphometry [17]. The following parameters were measured: thickness of the molecular and granular layers (perpendicular to the pial surface at the apex of the folium, 10 measurements per animal); density of granule cells per 0.01 mm² of the granular layer; linear density of Purkinje cells (number of cells with a visible nucleus per 1 mm of the Purkinje cell layer); area of the soma and nucleus of Purkinje cells (at least 50 cells per animal, sectioned through the nucleolus); optical density of the Nissl substance in the Purkinje cell cytoplasm (relative units, Nissl-stained sections). Purkinje cells were classified as normochromic, hypochromic (with signs of chromatolysis), hyperchromic shrunken, and ghost cells (cell shadows with lysed nucleus), and the share of each type was calculated from no fewer than 100 cells per animal. Measurements were performed blind to group allocation.

Classification of Purkinje cells. Normochromic cells had a pear-shaped body, a central round nucleus with a distinct nucleolus and evenly distributed lumps of Nissl substance. Hypochromic cells were enlarged and pale, with peripheral, central or total dissolution of the Nissl substance (chromatolysis) and, in some cells, an eccentric nucleus. Hyperchromic cells were reduced in size, with an angular contour, intensely and homogeneously stained cytoplasm, a pyknotic nucleus and a corkscrew-shaped apical dendrite. Ghost cells were pale, structureless cell outlines with a lysed or absent nucleus. Empty beds in the Purkinje cell row and figures of neuronophagia (a neuron surrounded by three or more glial cells) were recorded separately.

Statistics. The animal was taken as the unit of analysis. Data are presented as the mean ± standard error of the mean (M ± m). The normality of distributions was checked with the Shapiro–Wilk test, and differences between each experimental subgroup and the control group were

assessed with Student's t-test for independent samples. Differences were considered statistically significant at $p < 0.05$.

Ethics. All manipulations complied with the European Convention for the Protection of Vertebrate Animals used for Experimental and Other Scientific Purposes (Strasbourg, 1986) [18] and national rules for the use of laboratory animals; the report follows the ARRIVE 2.0 guidelines [19].

RESULTS AND DISCUSSION

In control animals the cerebellar cortex had a typical three-layered structure. Purkinje cells were arranged in a regular single row, had pear-shaped bodies, a centrally located light nucleus with a distinct nucleolus and evenly distributed coarse lumps of Nissl substance. Vessels of the pia mater and the cortex were of moderate blood filling, and perivascular and pericellular spaces were narrow.

One hour after stress the leading changes were vascular: venous plethora of pial and intracortical vessels, dilated capillaries and widening of the perivascular and pericellular spaces. The molecular layer was loosened and thickened (Table 1). Many Purkinje cells were swollen and pale, with peripheral chromatolysis; the share of normochromic cells had already decreased to 84.3 ± 1.4% (Table 3). The linear density of Purkinje cells did not differ significantly from the control.

After 24 hours the changes reached their maximum. Oedema of the molecular layer and of the Purkinje cell layer was most pronounced; single diapedetic microhaemorrhages appeared. Purkinje cells were heterogeneous: alongside swollen cells with total chromatolysis and eccentric nuclei there were shrunken hyperchromic cells with pyknotic nuclei and corkscrew-shaped apical dendrites, as well as ghost cells. In the granular layer, focal loosening and widening of the spaces around the glomeruli were noted, while most granule cells retained their normal appearance.

After 72 hours oedema decreased, but destructive changes in Purkinje cells persisted. Shrunken hyperchromic cells and ghost cells were frequent, gaps ("empty beds") appeared in the Purkinje cell row, and satellite glial cells and Bergmann glia became more prominent; single figures of neuronophagia were seen. *By day 7* oedema and plethora had largely resolved and most Purkinje cells were normochromic, but empty beds and moderate glial proliferation in the Purkinje cell layer remained.

Table 1

Thickness of the cerebellar cortex layers and granule cell density after acute stress (M ± m)

Parameter	Control (n = 10)	Experimental subgroups: time after stress (n = 5 each)			
		1 h	24 h	72 h	7 days
Molecular layer thickness, µm	201.1±3.2	216.6±2.7**	221.2±4.9**	205.5±3.6	200.9±2.5
Granular layer thickness, µm	237.5±6.6	247.6±5.8	244.9±5.4	250.2±4.0	224.8±4.9
Granule cell density,	313.2±9.7	321.1±10.1	290.2±7.0	300.6±8.6	288.0±14.0

per 0.01 mm²					

Note: * p < 0.05; ** p < 0.01; *** p < 0.001 compared with the control group (Student's t-test).

Morphometry confirmed the visual impression. The thickness of the molecular layer increased by 7.7% 1 h after stress (p < 0.01) and by 10.0% after 24 h (p < 0.01), and returned to the control level by 72 h (Table 1, Fig. 1). Since the number of cells in this layer is small, the transient thickening is best explained by interstitial and pericellular oedema rather than by structural growth. The thickness of the granular layer and the density of granule cells did not change significantly at any time point; only a tendency towards a decrease in granule cell density (by 7.3%–8.0%) was recorded at 24 h and 7 days.

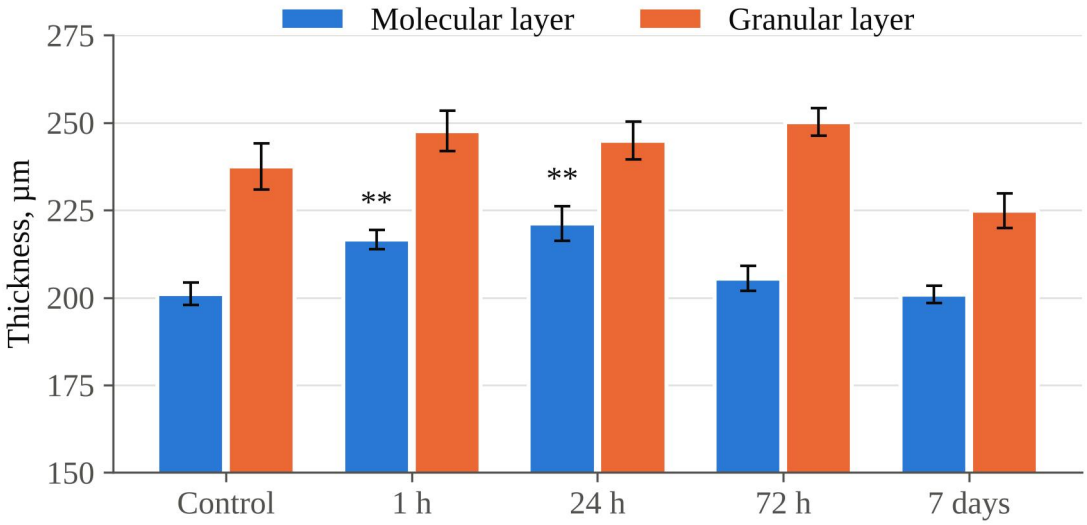


Fig. 1. Thickness of the molecular and granular layers of the cerebellar cortex at different times after acute stress (M ± m). ** p < 0.01 vs. control.

Purkinje cells responded most strongly (Table 2, Fig. 2). Their linear density did not change at 1 h but decreased by 18.1% at 24 h (p < 0.01) and by 19.3% at 72 h (p < 0.01); on day 7 it remained 12.4% below the control (p < 0.05). The dynamics of the soma area were biphasic: an increase up to 406.9 µm² at 24 h (+15.8%, p < 0.01) reflected cytoplasmic swelling, whereas at 72 h the soma area fell below the control level (−12.5%, p < 0.05) owing to the accumulation of shrunken hyperchromic cells. The nuclear area decreased significantly at 72 h (−12.7%) and 7 days (−8.7%), consistent with nuclear condensation. The optical density of the Nissl substance fell as early as 1 h after stress (−28.1%, p < 0.01), stayed low up to 72 h and recovered by day 7, indicating that chromatolysis is an early and largely reversible reaction.

Table 2

Morphometric parameters of cerebellar Purkinje cells after acute stress (M ± m)

Parameter	Control (n = 10)	Experimental subgroups: time after stress (n = 5 each)			
		1 h	24 h	72 h	7 days
Linear density,	32.5±1.1	31.1±1.2	26.6±0.7**	26.2±0.8**	28.4±0.5*

cells/mm					
Soma area, μm²	351.4±9.8	371.9±6.8	406.9±9.3**	307.5±6.6*	344.2±9.2
Nuclear area, μm²	95.2±1.9	93.1±3.4	100.2±3.8	83.1±2.1**	86.9±3.3*
Optical density of Nissl substance, rel. units	0.42±0.02	0.30±0.02**	0.29±0.02**	0.27±0.02**	0.39±0.02

Note: * $p < 0.05$; ** $p < 0.01$; *** $p < 0.001$ compared with the control group (Student's t-test).

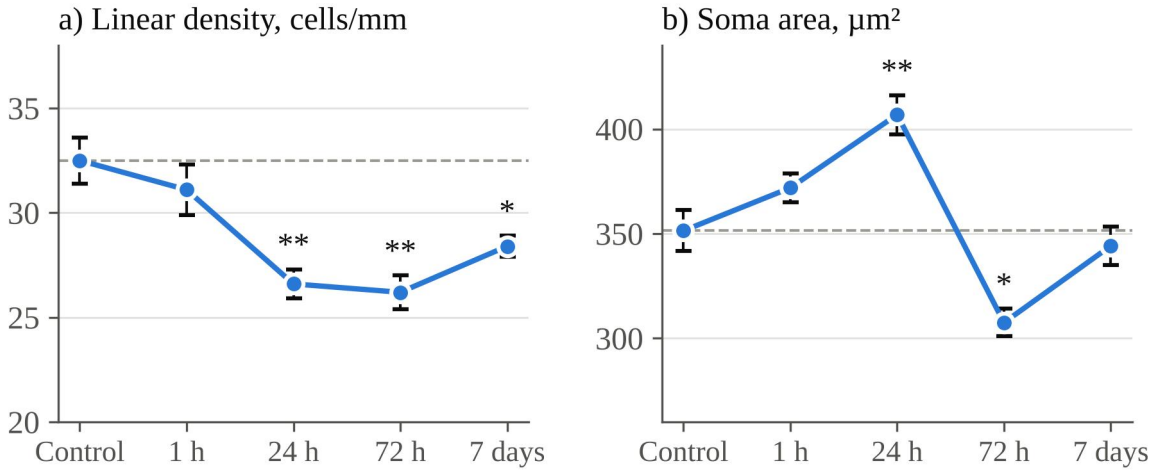


Fig. 2. Dynamics of the linear density (a) and soma area (b) of Purkinje cells after acute stress (M ± m; dashed line — control level). * $p < 0.05$; ** $p < 0.01$ vs. control.

Analysis of the Purkinje cell population revealed a shift from normochromic to altered forms (Table 3, Fig. 3). The share of normochromic cells decreased from 94.0 ± 0.8% in the control to 56.4 ± 1.8% at 24 h ($p < 0.001$). Hypochromic cells with chromatolysis and hyperchromic shrunken cells reached their maximum at 24 h (22.1 ± 1.0% and 18.0 ± 2.3%, respectively), whereas the share of ghost cells continued to grow and was highest at 72 h (4.2 ± 0.5%), reflecting the transition from reversible to irreversible damage. By day 7 the share of normochromic cells recovered to 86.2 ± 2.4%, but ghost cells were still more frequent than in the control (2.1 ± 0.2% vs. 0.6 ± 0.2%, $p < 0.001$).

Table 3

Distribution of Purkinje cells by morphological type after acute stress, % (M ± m)

Parameter	Control (n = 10)	Experimental subgroups: time after stress (n = 5 each)			
		1 h	24 h	72 h	7 days
Normochromic	94.0±0.8	84.3±1.4***	56.4±1.8***	68.3±3.3***	86.2±2.4**
Hypochromic (chromatolysis)	2.5±0.3	7.6±0.9***	22.1±1.0***	15.2±2.1***	6.7±1.7**

Hyperchromic (shrunken)	2.8±0.6	7.4±0.5***	18.0±2.3***	12.4±1.9***	4.9±1.3
Ghost cells	0.6±0.2	0.7±0.3	3.5±0.4***	4.2±0.5***	2.1±0.2***

Note: * $p < 0.05$; ** $p < 0.01$; *** $p < 0.001$ compared with the control group (Student's t-test).

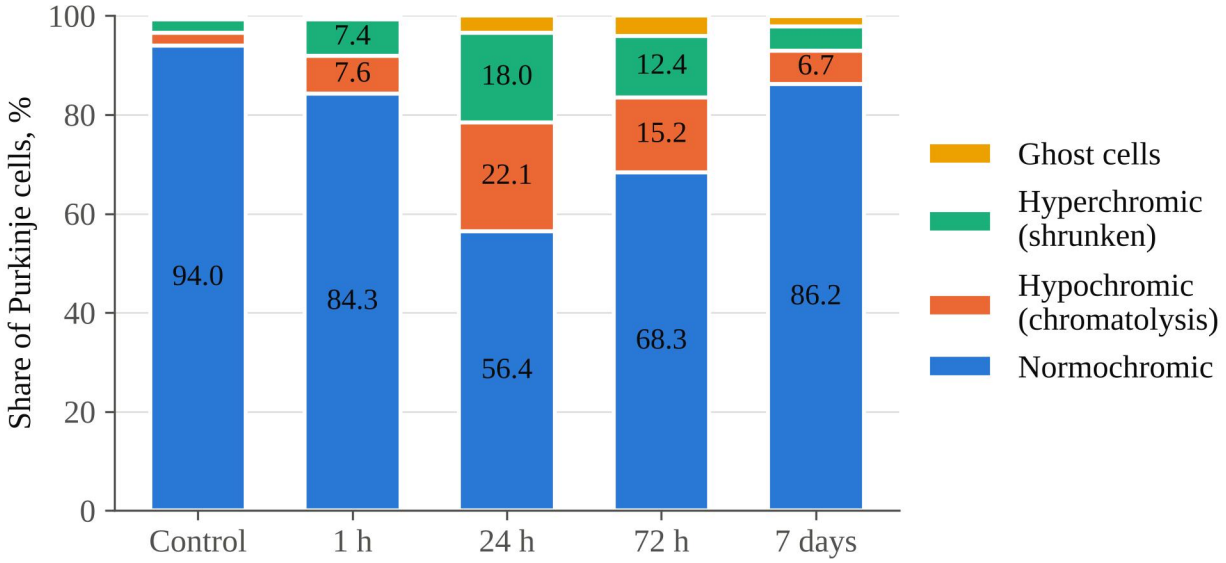


Fig. 3. Distribution of Purkinje cells by morphological type at different times after acute stress, % of counted cells.

The results obtained show that a single 2-hour immobilization triggers in the cerebellar cortex a sequence of changes that can be divided into three phases. The first, reactive (vascular-oedematous) phase, occupying the first 24 hours, is characterized by plethora, perivascular and pericellular oedema, swelling of Purkinje cells and chromatolysis without a significant loss of neurons. The second, destructive phase (24–72 h) is marked by a decrease in Purkinje cell density, the accumulation of hyperchromic and ghost cells and the activation of glia. The third, reparative-compensatory phase (by day 7) is characterized by the regression of oedema and the restoration of most Purkinje cells, against the background of a persistent partial loss of these neurons and moderate gliosis.

The early vascular-oedematous changes are in line with data showing that acute stress increases the permeability of the blood–brain barrier through activation of brain mast cells [13] and that one day of restraint already causes damage to capillary endothelium and swelling of astrocytic end-feet [14]. The molecular layer, with its dense neuropil and Bergmann glial processes, appears to be the region where such oedema is most readily recorded morphometrically.

Two components can be distinguished in the oedema observed. The early widening of perivascular spaces, combined with plethora and diapedetic microhaemorrhages, points to a vasogenic component associated with increased endothelial permeability, whereas the swelling of Purkinje cell bodies and pericellular clearing suggest a cytotoxic component caused by the failure of ion pumps under energy deficit. Both components largely resolve within 72 h, which explains the return of molecular layer thickness to control values.

The selective vulnerability of Purkinje cells compared with granule cells is consistent with their functional characteristics. Purkinje cells express glucocorticoid receptors [10], have a very high energy demand and receive powerful excitatory input from climbing fibres [11]. Under excess glucocorticoids and catecholamines, energy supply is reduced while glutamatergic stimulation and intracellular calcium increase [4], creating conditions for chromatolysis and, in the most affected cells, for irreversible condensation of the cytoplasm and nucleus. The decrease in the number and size of Purkinje cells described in chronic stress [12] is thus already outlined, in a less pronounced and partly reversible form, after a single acute exposure.

Comparison with chronic models highlights the specific features of the acute response. In rats exposed to 10 days of multiple sequential stressors, Rajaei et al. found a significant decrease in the number and size of Purkinje cells without a change in molecular layer thickness [12]. In our acute model, by contrast, the reduction of soma area was preceded by swelling, and the thickening of the molecular layer was transient. The early response is therefore dominated by oedema and potentially reversible dystrophy, whereas cell loss and shrinkage become the leading features only after 24–72 h.

Hyperchromic ("dark") neurons deserve separate comment. Some of them may represent a reversible state or a fixation artefact, whereas the appearance of ghost cells and empty beds indicates a true loss of neurons. The persistence of reduced Purkinje cell density on day 7, despite the normalization of soma area and Nissl substance, suggests that part of the population is lost irreversibly, while the surviving cells restore their structure. The growth of satellite glia and Bergmann glia at 72 h–7 days is consistent with the reactive role of astrocytes in limiting damage and remodelling the tissue [20].

The changes found have functional significance. Purkinje cells integrate signals from a huge number of parallel fibres and from a climbing fibre and provide the only output of the cerebellar cortex, which inhibits the deep cerebellar nuclei [11]. Chromatolysis, which reflects a reduction in protein synthesis, and a 12.4%–19.3% decrease in Purkinje cell density are expected to weaken this inhibitory control and to impair the timing and precision of movements, which clinically corresponds to unsteadiness, impaired balance and tremor. Given the connections of the cerebellum with the ventral tegmental area and the limbic system [7, 8], the same changes may contribute to post-stress anxiety and depression-like behaviour. Behaviour was not assessed in this experiment; correlating morphometric data with motor tests (rotarod, beam walking) is a task for the next stage of the work.

From a practical point of view, the quantitative criteria used here (Purkinje cell linear density, soma and nuclear area, Nissl substance density and the ratio of Purkinje cell types) are simple to obtain on routinely stained sections and can be used to compare the severity of stress-induced damage in different experimental conditions, including the evaluation of protective agents.

The sequence of the assessment is summarized as an algorithm (Fig. 4) that can be used in experimental studies of stress and of neuroprotective agents. The study has limitations: the subgroups are small (n = 5), the glial response was assessed only by histological stains, and electron microscopy was not performed. Immunohistochemistry (GFAP, Iba-1, calbindin) and ultrastructural analysis are planned for the next stage of the dissertation research.

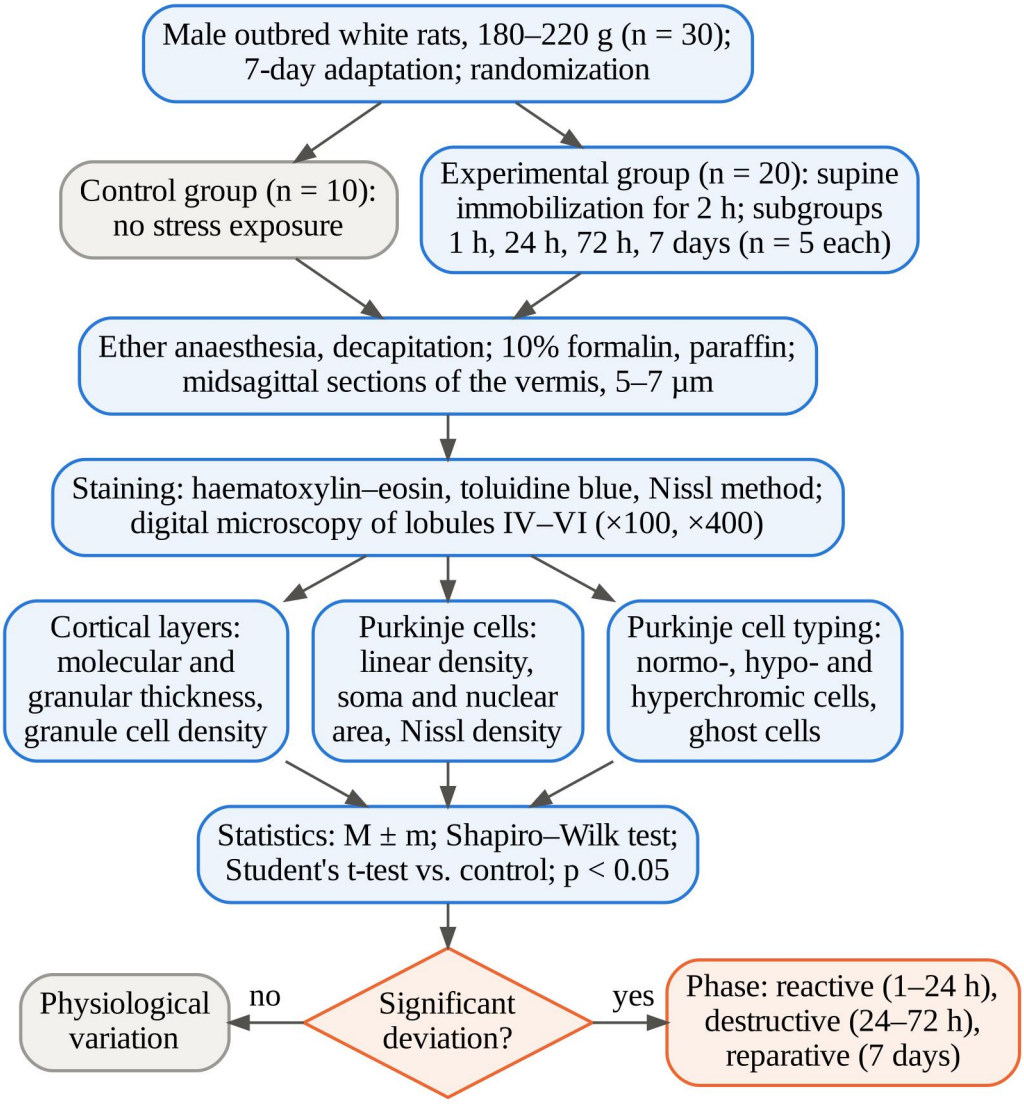


Fig. 4. Algorithm of the histological and morphometric assessment of the cerebellum in acute stress.

CONCLUSIONS AND RECOMMENDATIONS

1. A single 2-hour immobilization stress causes phase-dependent changes in the rat cerebellar cortex: a reactive vascular-oedematous phase (1–24 h), a destructive phase (24–72 h) and a reparative-compensatory phase (by day 7).
2. Purkinje cells are the most vulnerable element of the cerebellar cortex: their linear density decreases by 19.3% at 72 h, and the share of normochromic cells falls to 56.4 ± 1.8% at 24 h; granule cells remain relatively resistant.
3. Swelling of the molecular layer, chromatolysis and the decrease in Nissl substance density are largely reversible, whereas the partial loss of Purkinje cells persists on day 7.
4. Linear density, soma and nuclear area of Purkinje cells, the optical density of Nissl substance and the ratio of Purkinje cell types are informative quantitative criteria for assessing stress-induced cerebellar damage.

Recommendations. In experimental studies of acute stress, morphological assessment of the cerebellum should include the 24–72 h interval, when destructive changes are maximal. This interval is also the rational window for testing antioxidants, neuroprotectors and adaptogens. The proposed algorithm (Fig. 4) can be used in research laboratories and in the teaching of morphology and pathophysiology.

REFERENCES

1. Selye H. A syndrome produced by diverse nocuous agents. Nature. 1936;138:32.
2. McEwen BS. Physiology and neurobiology of stress and adaptation: central role of the brain. Physiol Rev. 2007;87(3):873–904.
3. Ulrich-Lai YM, Herman JP. Neural regulation of endocrine and autonomic stress responses. Nat Rev Neurosci. 2009;10(6):397–409.
4. Sapolsky RM, Romero LM, Munck AU. How do glucocorticoids influence stress responses? Integrating permissive, suppressive, stimulatory, and preparative actions. Endocr Rev. 2000;21(1):55–89.
5. Lupien SJ, McEwen BS, Gunnar MR, Heim C. Effects of stress throughout the lifespan on the brain, behaviour and cognition. Nat Rev Neurosci. 2009;10(6):434–445.
6. Schmahmann JD, Sherman JC. The cerebellar cognitive affective syndrome. Brain. 1998;121(4):561–579.
7. Moreno-Rius J. The cerebellum under stress. Front Neuroendocrinol. 2019;54:100774.
8. Baek SJ, Park JS, Kim J, Yamamoto Y, Tanaka-Yamamoto K. VTA-projecting cerebellar neurons mediate stress-dependent depression-like behaviors. eLife. 2022;11:e72981.
9. Gheorghe DA, Panouillères MTN, Walsh ND. Psychosocial stress affects the acquisition of cerebellar-dependent sensorimotor adaptation. Psychoneuroendocrinology. 2018;92:41–49.
10. Pavlík A, Buresová M. The neonatal cerebellum: the highest level of glucocorticoid receptors in the brain. Brain Res. 1984;314(1):13–20.
11. Ito M. Cerebellar circuitry as a neuronal machine. Prog Neurobiol. 2006;78(3–5):272–303.
12. Rajaei F, Akhavan Tavakkoli M, Azhdari-Zarmehri H. Studying of chronic multiple sequential stress effects on microscopic structure of cerebellar cortex in male rat. J Birjand Univ Med Sci. 2012;19(4):355–361.
13. Esposito P, Gheorghe D, Kandere K, Pang X, Connolly R, Jacobson S, Theoharides TC. Acute stress increases permeability of the blood–brain barrier through activation of brain mast cells. Brain Res. 2001;888(1):117–127.
14. Sántha P, Veszelka S, Hoyk Z, Mészáros M, Walter FR, Tóth AE, et al. Restraint stress-induced morphological changes at the blood-brain barrier in adult rats. Front Mol Neurosci. 2016;8:88. doi:10.3389/fnmol.2015.00088.
15. Buynitsky T, Mostofsky DI. Restraint stress in biobehavioral research: recent developments. Neurosci Biobehav Rev. 2009;33(7):1089–1098.
16. Paxinos G, Watson C. The Rat Brain in Stereotaxic Coordinates. 7th ed. San Diego: Academic Press; 2013.
17. Avtandilov GG. Meditsinskaya morfometriya [Medical morphometry]. Moscow: Meditsina; 1990. 384 p. (In Russ.)
18. Council of Europe. European Convention for the Protection of Vertebrate Animals used for Experimental and Other Scientific Purposes (ETS No. 123). Strasbourg; 1986.

19. Percie du Sert N, Hurst V, Ahluwalia A, Alam S, Avey MT, Baker M, et al. The ARRIVE guidelines 2.0: updated guidelines for reporting animal research. PLoS Biol. 2020;18(7):e3000410.
20. Sofroniew MV, Vinters HV. Astrocytes: biology and pathology. Acta Neuropathol. 2010;119(1):7–35.